JOURNAL OF MATERIALS SCIENCE **37** (2002) 1635–1644

J-R curve determination of magnesium hydroxide filled polypropylene using the normalization method

C. MORHAIN, J. I. VELASCO*
Centre Català del Plàstic (CCP), Universitat Politècnica de Catalunya (UPC), C/Colom 114, E-08222 Terrassa (Barcelona), Spain
E-mail: jose.ignacio.velasco@upc.es

The normalization method is applied to different magnesium hydroxide filled polypropylenes. As the load separation principle is the basis of the method, its validity is checked using the load separation criterion developed by Sharobeam and Landes. Load separability is checked for all the materials when the condition of stationary crack length is fulfilled. During the determination of the deformation function using the normalization method, the large decrease of the load value of highly filled materials make it impossible to describe the load normalization variation with plastic displacement by a power law equation. Nevertheless, for the lower-filled materials, i.e. up to 40 wt% with copolymer PP and 20 wt% with homopolymer PP, the *J-R* curve can be determined and high concordance is found with the *J-R* curve obtained by multiple specimen method. The applicability of the normalization method is discussed in terms of the geometry of the plastic deformation zone. It is found that the materials that are not suitable for normalization method application are characterized by a very small plastic zone, due to the restriction of plastic flow caused by mineral filler.

1. Introduction

Particulate-filled polypropylene materials represent an increasing part of the polymeric materials market, thanks to the modification of the properties of the polypropylene matrix due to the incorporation of rigid particles. Higher stiffness, lower post-molding shrinkage, better superficial appearance are some of the improvements related to the mineral filler presence. Nevertheless, it appeared that dispersed rigid particles might also involve important modifications of the mechanical behavior of the material and especially of its fracture resistance. For this reason, numerous studies were dedicated to the fracture resistance of polypropylene filled with particulate mineral fillers as talc, calcium carbonate, glass beads, inorganic flame retardants, etc.

In a recent paper [1], the load normalization method developed by Herrera and Landes [2] was successfully applied to unfilled copolymeric polypropylenes and the resistance curves J-Δa of these materials were determined. In fact, at low strain rate, fracture resistance of PP-based materials is generally characterized through the use of the J-integral concept developed by Rice [3], due to the important plastic deformation that appears during the fracture process of this kind of materials. The determination of a critical value of J-integral is generally performed through the construction of the resistance curve J-Δa of the material. The method commonly used for this purpose is the multiple specimen method developed by Begley and Landes [4], which involves the testing of an important number of specimens. For this reason, considerable efforts were dedicated to the development of a lower time and material consumption method for determining the *J-R* curve. In this sense, the normalization method allowed the construction of the resistance curve from the record of a single fracture test. This method is based on the assumption that load can be separated into two independent and multiplicative functions, namely the geometry function and the deformation function, which depend only of the crack length and the plastic displacement, respectively. Although load separation was analytically checked for Ramberg-Osgood materials using the EPRI handbook solutions [5], its validity for other materials was only experimentally checked for a few metallic and plastic materials [6–11]. The work of Sharobeam and Landes [6] resulted in the definition of a criterion, which allows the load separation validity to be experimentally checked. Once load separation has been checked, the normalization method can be applied in order to determine the value of the crack length increment, Δa. This method was successfully applied for several materials, of metallic [6, 7] or polymeric nature [8–11]. Nevertheless, no works have been published about load

*Author to whom all correspondence should be addressed.

separation validity and normalization method application for systems of polymeric matrix and rigid particulate fillers.

The aim of the present work is the study of the applicability of the load normalization method for the determination of the *J-R* curve of several magnesium hydroxide-filled polypropylenes. As a first step, the validity of load separation principle is checked using the separation criterion defined by Sharobeam and Landes and the geometry function is determined for each material. The load can then be normalized and the deformation function is determined. Once both functions are known, the value of the crack length increment can be determined at any instant of the test and the J-Δa curve can be plotted. The validity of the method is evaluated comparing the resulting *J-R* curves with those obtained by the traditional multiple specimen method.

2. Theoretical background

2.1. Load separation criterion

The load separation principle considers that load can be separated in two multiplicative and independent functions:

$$P = G(a/W) \times H(v_{pl}/W) \tag{1}$$

where a, v_{pl} and W are the crack length, the plastic displacement and the specimen width, respectively, and G and H are the so-called geometry and deformation functions.

The load separation criterion developed by Sharobeam and Landes [6] defines the load separation parameter, S_{ij}, as the ratio between the load values at the same plastic displacement level for two notched specimens with different notch depths:

$$S_{ij} = \left.\frac{P(a_i, v_{pl})}{P(a_j, v_{pl})}\right|_{v_{pl}} \tag{2}$$

From Equations 1 and 2, the separation parameter is defined as:

$$S_{ij} = \left.\frac{G(a_i/W)}{G(a_j/W)}\right|_{v_{pl}} \tag{3}$$

The separation criterion considers that, when the crack lengths remain constant, load is separable if the separation parameter value remains constant during the whole plastic displacement range.

Once the validity of the load separation principle is checked, the deformation function $G(a/W)$ can be determined. The functional relationship between the geometry function and the ligament length, $b = W - a$, can be determined from the study of the variations of the separation parameter with ligament length, considering that, for a same reference sample j, the separation parameter and the geometry function are directly proportional:

$$S_{ij} = C_1 \cdot G(b_i/W), \text{ for constant } (b_j/W) \tag{4}$$

where C_1 is the proportionality constant. The functional relationship between the geometry function and the ligament length can thus be determined through the graphic representation of S_{ij} vs b_i/W, which can be generally fitted by a power law equation:

$$S_{ij} = C_2 \cdot (b_i/W)^{C_3} \tag{5}$$

where C_2 and C_3 are constants.

The η_{pl} geometric factor can then be determined from these results using the analytical form obtained by Sharobeam and Landes [6] from the derivation of the separable form:

$$\eta_{pl} = \frac{\mathrm{d}G(b/W)/\mathrm{d}(b/W)}{G(b/W)}\frac{b}{W} \tag{6}$$

It results, from Equations 4–6, that:

$$\eta_{pl} = C_3 \tag{7}$$

For the SENB geometry, the η_{pl} value is theoretically equal to 2.

2.2. Normalisation method

Once load separation validity has been checked and the geometry function is known, normalized load can be defined as:

$$P_N = \frac{P}{G(a/W)} \tag{8}$$

The deformation function $H(v_{pl}/W)$ can thus be determined from the graphic representation of normalized load versus normalized plastic displacement, v_{pl}/W, as illustrated in Fig. 1. The determination of the relationship between normalized load and normalized

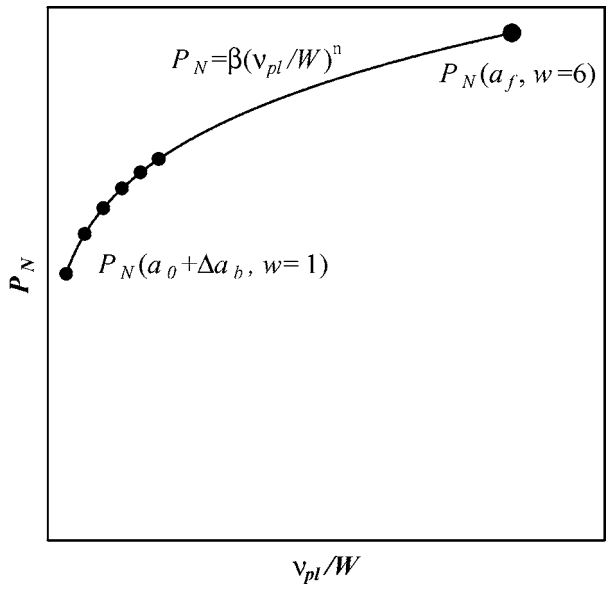

Figure 1 Graphic determination of the functional expression of the deformation function. w is the weight of each individual point for the power law fit.

plastic displacement requires the emission of a hypothesis about its functional form. Several expressions were suggested in literature to describe the variations of the deformation function. Originally, the functional form used by Landes and Herrera [2] followed a power law expression:

$$H(v_{pl}/W) = \beta(v_{pl}/W)^n \tag{9}$$

Although good results were obtained with this expression [2, 9, 12, 13], it was reported that a better accuracy was obtained for the initial region of the *J-R* curve when a combination of a power law and a straight line were used [14]. These results encouraged the utilization of the so-called LMN function, as defined by Orange [15]. In the present work, normalized load is fitted by a power law. In a recent work [1], good agreement was obtained with this functional form for unfilled PP. The power law fit is performed from six points of the early separable region and the final point of the test. The determination of both normalized load and normalized plastic displacement are performed considering, for the initial region, the initial crack length a_0 corrected by a crack length increment, Δa_b, corresponding to crack tip blunting. On the other hand, the final point is determined using the final length of the crack, measured directly on the surface fracture of the specimen. It was observed that it is important to give a higher weight to the final point during the fit [1]. A weight six times higher than that of the points of the initial region is used here.

Once both geometry and deformation functions are known, the value of Δa can be determined at any instant from the value of P and d of the fracture records. On the other hand, the value of J-integral is obtained from the approximate equation developed by Rice [3]:

$$J_0 = \frac{\eta U}{B(W - a_0)} \tag{10}$$

where U is the area under the load-displacement curve and η is the overall factor ($\eta = \eta_{el} = \eta_{pl}$, in the present case). The correction for propagating cracks was applied:

$$J = J_0\left(1 - \frac{\Delta a}{2(W - a_0)}\right) \tag{11}$$

Once the values of J-integral and crack length increment are known, the *J-R* curve can be plotted.

3. Materials

Two polypropylene grades, kindly supplied by Repsol Química S.A. (Spain), were used. Isplen PP050 is a homopolymer polypropylene and Isplen PB140 is a block copolymer grade with an 8–9% of ethylene. Both grades are suitable for injection-molding process. The basic characteristics of these polymers are shown in Table I.

Two different magnesium hydroxide grades, kindly supplied by Martinswerk GmbH (Germany), were used: Magnifin H5 is a grade of high purity with a particle size of 1.4 μm and free of any superficial coating. Magnifin H5L is a grade similar to Magnifin H5 but with a surface coating based on polymeric substance.

TABLE I Composition and basic characteristics of the materials under study

Material	Matrix	Filler	Filler Content (wt%)	MFI[a] (g/10 min)	HDT[b] (°C)
HPP	Isplen PP050	Magnifin H5	0	5.73	70.3
H2H5			2	5.37	80.0
H10H5			10	5.14	93.1
H20H5			20	4.58	112.5
H40H5			40	3.46	115.1
H60H5			60	0.66	123.8
BPP	Isplen PB140	Magnifin H5L	0	3.33	54.2
B40H5L			40	3.24	66.7
B60H5L			60	1.65	74.0

[a]Measured at 230°C with 2160 g.
[b]Measured at 120°C/h with 1.8 MPa.

Compounding was performed using a Collin corrotating twin-screw extruder with a L/D ratio of 24 and a screw diameter of 25 mm. The temperature of the die was 195°C and the screw speed fixed at 60 rpm. The extrudate was cooled in water and pelletized. The composition of the different prepared materials is shown in Table I.

Prismatic bars with nominal dimensions $6.35 \times 12.7 \times 127$ mm^3 were injection-molded using a Mateu y Solé (Spain) 440-90 injection machine. The nominal injection pressure was 100 MPa and the temperature of the melt 195°C. All the specimens were annealed at 110°C during 24 hours in order to release the residual stresses. Any deformed specimen was rejected.

4. Experimental procedure

The tests were performed following the procedure suggested by the ESIS for the multiple specimen method [16]. The test configuration used for the present study was three-point bending. Single Edge Notched Bending (SENB) specimens were obtained by cutting the injected prismatic bars into halves. The final dimensions were $B \times W \times L = 6.35 \times 12.7 \times 63.5$ mm^3. A notch was inserted centrally in the narrowest side of the specimens, using a 45° V notch broaching tool with a notch tip radius of 0.25 mm.

The study of load separation validity was carried out performing tests on blunt-notched specimens, in order to get stationary cracks and thus to retard the fulfil the stationary cracks condition. On the other hand, the fracture tests used for the application of normalization method were performed on precracked specimen. These specimens were obtained by sharpening the blunt notches with a single cut from a razor blade.

The materials based on homopolymer PP were tested using an INSTRON 4507 universal testing machine with a load cell of 1 kN. The fracture test records used for the application of the normalization method to the block copolymer-based materials were records obtained during a previous study [17], using an ADAMEL DY-30 testing machine. All the tests were performed at loading speed of 1 mm/min and at room temperature.

5. Results and discussion

5.1. Application of load separation criterion

The load-displacement records obtained during the three-point bending test of blunt-notched specimens are shown in Fig. 2. As recommended by the ESIS protocol, indentation of the rolls was subtracted of the values of displacement.

It is worth noting that unstable fracture occurs in the case of unfilled and 2 wt%-filled homopolymer PP (HPP and H2H5). This phenomenon has been also observed in other works [18, 19]. Moreover, stable crack propagation is observed in almost all of the other homopolymeric based-materials.

From the load-displacement records, plastic displacement is determined using Equation 12:

$$v_{pl} = d - v_{el} = d - C(a/W) \times P \qquad (12)$$

where v_{el} is the elastic component of the displacement, which can be calculated using the expression of the compliance $C(a/W)$ [20]:

$$C\left(\frac{a}{W}\right) = \frac{1}{E \times B} \times \left(\frac{S}{W-a}\right)^2 \times \left[1.193 - 1.98\left(\frac{a}{W}\right) + 4.478\left(\frac{a}{W}\right)^2 - 4.443\left(\frac{a}{W}\right)^3 + 1.739\left(\frac{a}{W}\right)^4\right] \qquad (13)$$

In this expression, S is the span of the test ($S = 50.8$ mm) and E is the Young's modulus of the material. For each fracture test, E is determined from the slope of the linear part of the load-displacement curve, which is equal to $1/C(a_0/W)$ and the initial value of crack depth, a_0.

Once plastic displacement is determined at any instant of the test, the separation parameter, S_{ij}, can be determined. As stable crack propagation is observed, the sample used as a reference in the calculus of S_{ij} is the sample with the highest crack depth. It results in a lower stored energy below the *P-d* curve and thus in a later crack propagation initiation and in a reduction of the possible deformation of the notch. The variations of the values of S_{ij} with plastic displacement are shown in Fig. 3.

As it is reported in all the publicated works dealing with load separation criterion, the separation parameter value is not constant at low plastic displacement values. This points to the existence of an unseparable region that is generally associated with the transition between elastic and plastic behavior.

Beyond this unseparable region, the separation parameter value remains constant and the load can be expressed by a separable form. At higher plastic displacement levels, different behaviors are observable. For unfilled and 2 wt%-filled homopolymer PP (HPP and H2H5), the separation parameter maintains a constant value till unstable fracture occurs. For the other materials, and with exception of the unfilled and 40 wt% filled copolymer (BPP and B40H5L), the stable crack propagation discussed above also appears in a decrease of the value of S_{ij}, once a critical value of plastic displacement is reached. It can be observed, moreover, that this critical plastic displacement decreases as filler concentration is increased. In the case of the 60 wt%-filled homopolymer (H60H5), it seems that the crack propagation occurs before that separation parameter reaches a constant value, resulting thus in a lack of separable region.

The obtained values of S_{ij} are used in order to determine the geometry factor η_{pl}. For this, the variations of the separation parameter with the normalized ligament length, b_i/W, are represented in Fig. 4.

According to Equation 5, the experimental data are fitted by a power law equation, where the exponent is equal to the value of η_{pl}. The obtained values and the correlation coefficients of the power law fit are shown in Table II. It is worth noting that, due to the reduced number of points used for the power law fit, the experimental error is important and each point has a considerable

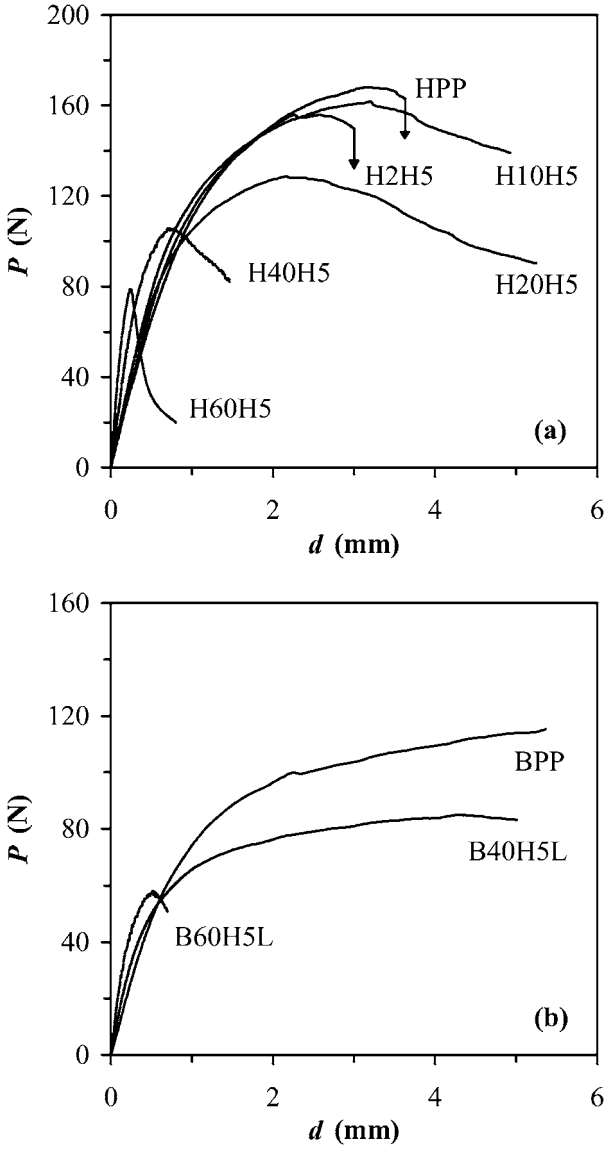

Figure 2 Load-displacement records obtained with blunt-notched specimens of (a) homopolymer and (b) block copolymer polypropylene based materials.

TABLE II Numerical values of η_{pl} obtained for the studied materials

Material	HPP	H2H5	H10H5	H20H5	H40H5	H60H5	BPP
η_{pl}	2.17	1.92	1.85	1.96	1.65	1.55	2.05
R^2	0.994	0.989	0.987	0.998	0.997	0.986	0.995

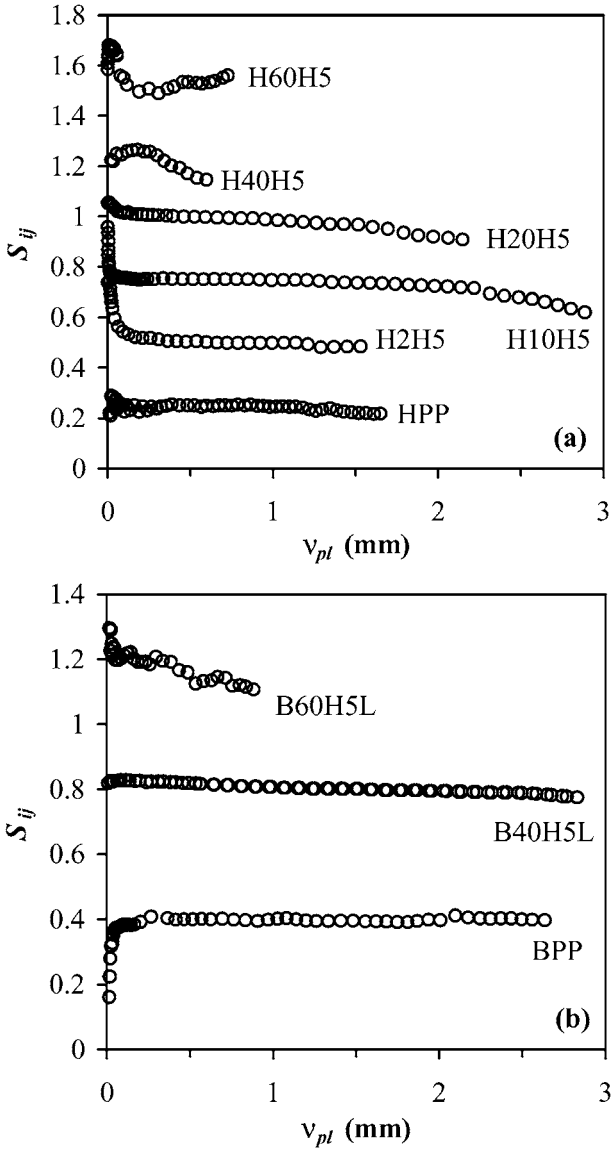

Figure 3 Variations of the separation parameter with plastic displacement. (a) HPP and (b) BPP based materials. Curves were translated along the Y-axis in order to avoid superpositions.

influence on the value of η_{pl}. For the materials filled with low content of $Mg(OH)_2$ (up to 20 wt%), the obtained values are close to the theoretical value of $\eta_{pl} = 2$ for the used SENB geometry. For the materials with higher filler concentrations, the obtained values are notably lower than the theoretical value although good correlation is found. The reduced number of points does not allow a correct discussion of the obtained values. Nevertheless, it is possible that the η_{pl} factor has a material dependence, as has been suggested by other workers [6].

For the following part of this study, the usual form of the geometry function,

$$G(b/W) = BW(b/W)^2 \tag{14}$$

is used, considering the theoretical value of η_{pl}.

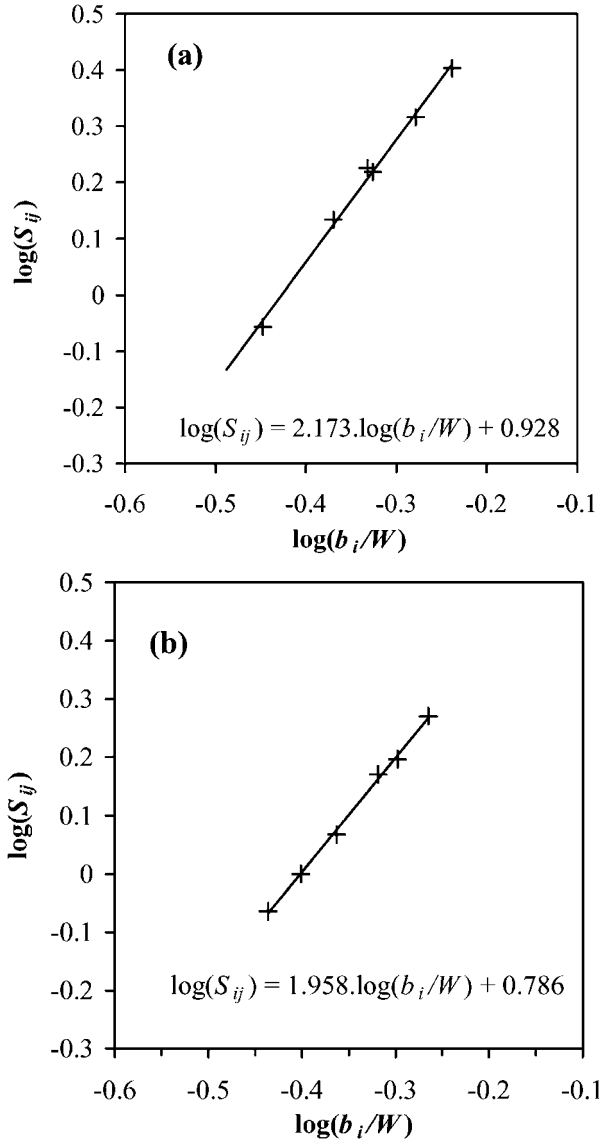

Figure 4 Variations of the separation parameter with the ligament length b_j for (a) BPP and (b) H20H5.

5.2. Application of load normalisation method

Once load separation has been checked for blunt-notched specimens, the normalization method can be applied. The use of load separation for pre-cracked specimens was demonstrated by Sharobeam and Landes [7] with the condition that crack propagation initiation occurs beyond the unseparable region, i.e. once the plastic deformation pattern has completely developed.

It is worth noting that, in the case of the unfilled homopolymer (HPP), unstable fracture occurs before any stable crack propagation appears. With low content of mineral filler, this unstable fracture disappears, due to the modification of the crystalline lattice by the filler nucleating action [21].

For the block-copolymer-based materials, the *J-R* curves obtained using the multiple specimen method [17] are shown in Fig. 5. The experimental data are fitted by a power law, according to ASTM [22].

One of the most ambiguous parts of the normalization method is the determination of the separable blunting region, i.e., the region where load is separable and crack

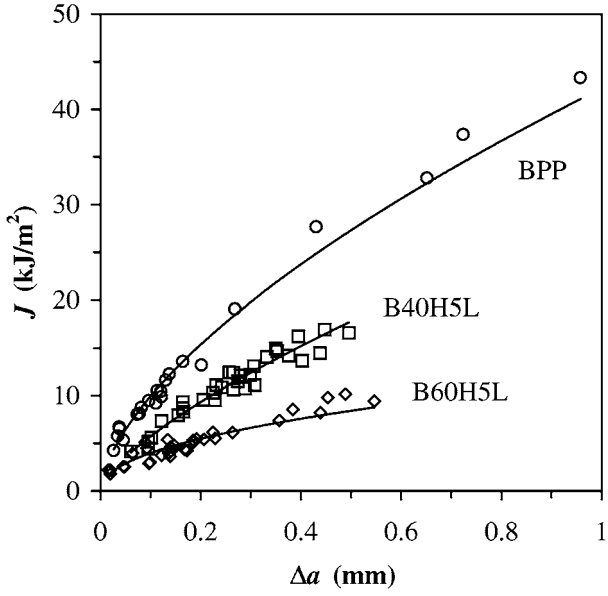

Figure 5 Resistance curves for the materials based on block copolymer PP and obtained by the multiple specimen method.

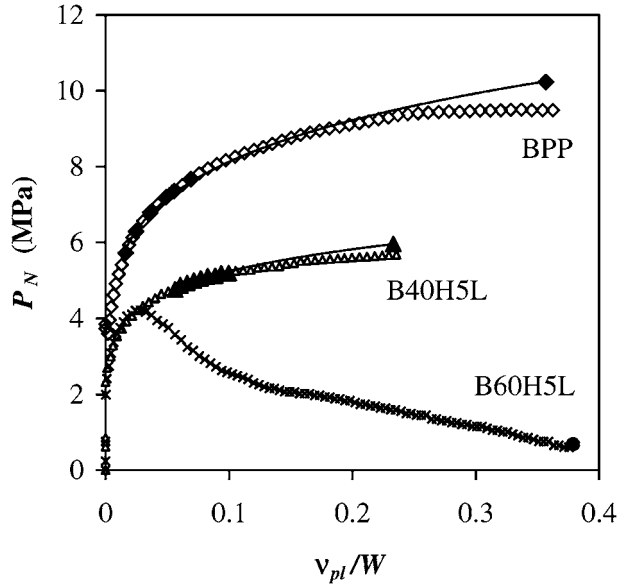

Figure 7 Graphic determination of the limits of the separable blunting region for the materials based on copolymer PP.

length increment is only due to crack tip blunting. In fact, the points belonging to this region correspond to one set of calibration points used for the determination of the deformation function expression. In order to determine the limits of this separable blunting region, $\nu_{pl\ \min}$ and $\nu_{pl\ \max}$, the variations of the separation parameter, S_{pb}, are represented in Fig. 6 for the three copolymer-based materials. This parameter is equivalent to the S_{ij} parameter defined above, with the difference that the p and b suffixes refer to a precracked and a blunt-notched specimen.

As reported for the variations of S_{ij}, the region of low plastic displacement is characterized by the noconstancy of the value of S_{pb}. Beyond this initial region, the separation parameter reaches a constant value. In fact, the value of S_{pb} slightly decreases due to crack tip blunting. At a certain plastic displacement, the decrease becomes more pronounced, due to the crack propagation. The separable blunting region lays between $\nu_{pl} = 0.3$ mm and $\nu_{pl} = 0.9$ mm for the unfilled block copolymer (BPP) and between $\nu_{pl} = 0.6$ mm and $\nu_{pl} = 1.3$ mm for the 40 wt% filled compound (B40H5L). It can be observed that increasing the mineral content of the material results in a shift of the separable blunting region to higher plastic displacement level. The variations of the separation parameter of the 60 wt% filled material (B60H5L) results in no separable blunting region where the value of S_{pb} is constant, due to the fact that the crack starts propagating within the early unseparable region. Moreover, it can be observed that the variations of the S_{pb} parameter are not monotonical, pointing to the concurrence between the crack propagation speeds of the precracked and the blunt-notched specimens.

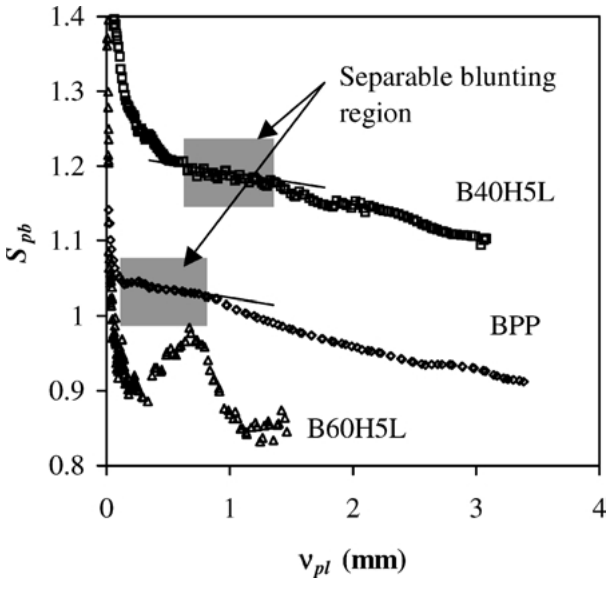

Figure 6 Variations of normalized load with normalized plastic displacement and determination of the deformation function. The power law fit is performed with the closed symbols.

The values of normalized load, P_N, and normalized plastic displacement, ν_{pl}/W, are calculated using Equations 8 and 14, and 12, respectively. The variations of P_N with ν_{pl}/W are shown in Fig. 7 considering an increment, Δa_b, corresponding to crack tip blunting, which is introduced using the blunting line equation:

$$\Delta a_b = \frac{J_0}{2m_{pcf}\sigma_y} \tag{15}$$

where σ_y is the tensile strength at yield, J_0 is the approximated J-integral value as defined in Equation 10 and m_{pcf} is the plastic constraint factor at the crack tip. A value of $m_{pcf} = \sqrt{3}$ is used in the present work, considering a tensional state predominantly of plane strain [23].

Meanwhile the power fit appears to be adequate for the unfilled and the 40 wt%-filled materials, the variations of the normalized load of the material filled with 60 wt% of magnesium hydroxide shows a trend totally different that the power law. In fact, the important decrease of the value of P after crack propagation initiation results in a value of P at the end of the test lower than the value of P at the early plastic deformation

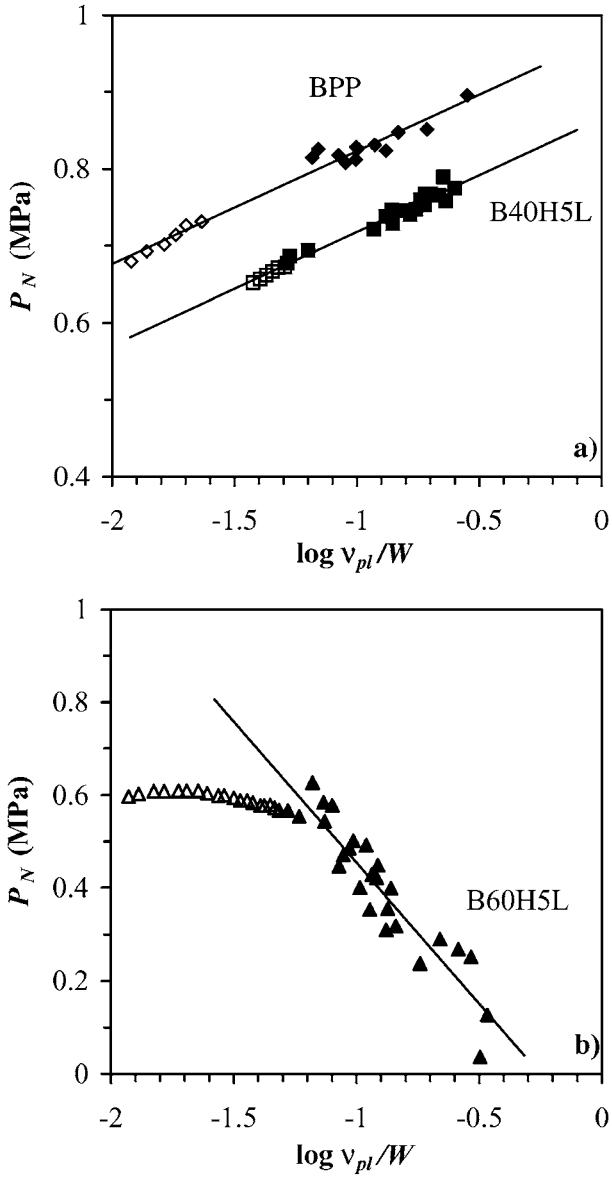

Figure 8 Graphic verification of the validity of the use of the power law fit for the unfilled and the 40 wt%-filled copolymer PP. Normalized load and plastic displacement are calculated from the final value of P, d and Δa of the multiple specimen tests (Closed symbols) and from the first points of the separable blunting region (Open symbols).

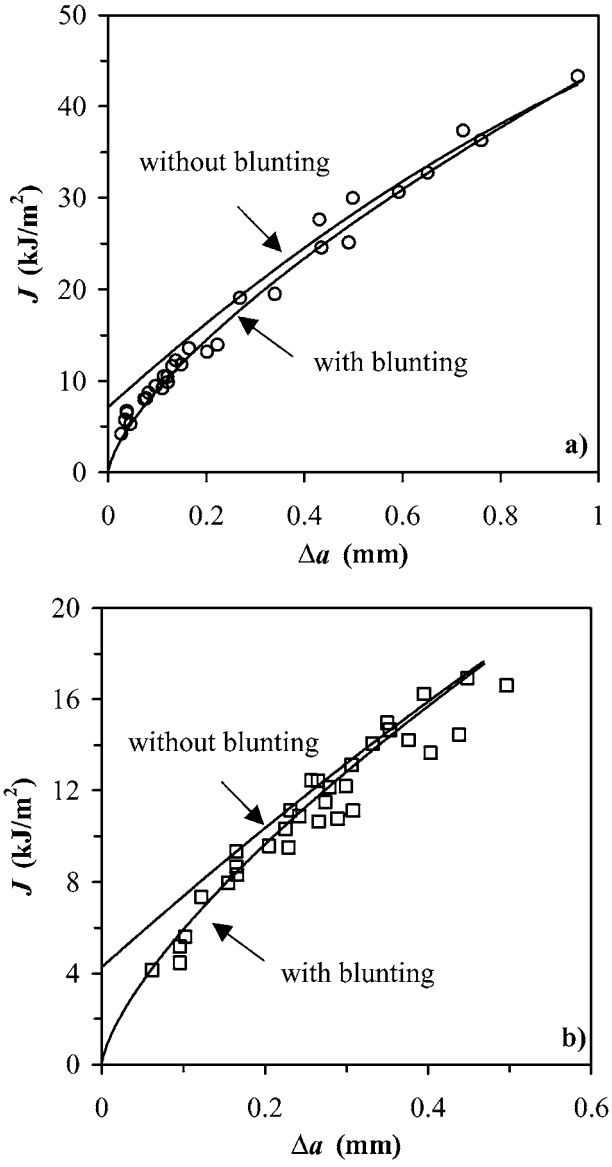

Figure 9 Resistance curves of (a) BPP and (b) B40H5L. Continuous lines were obtained by the normalization method and closed symbols are obtained by the multiple specimen method.

stage. If we consider that, before crack propagation starts, normalized load increases with plastic displacement, it is worth noting that, if a power law can follow either an increasing or a decreasing trend, it cannot describe both behavior with the same expression. Note also that the LMN function defined above is also a monotonic function.

In order to check the validity of the use of a power law fit, the value of P_N and v_{pl}/W obtained for the final point of all the multiple specimen fracture records are reported in Fig. 8. These points were calculated using the values of P_f, d_f and Δa_f.

The separable blunting region obtained for one of the samples is also represented. In the case of BPP and B40H5L, the experimental data are correctly fitted by a power law equation along the entire plastic displacement range. In the case of B60H5L, the separable blunting region is not represented, as this region cannot be determined. Although the experimental data can be approximately fitted by a power law, its trend is opposite to the trends of the other two materials, as the value of the normalized load decreased with plastic displacement. It can then be concluded that, for the 60 wt% filled material, the normalization method cannot be applied due to the lack of calibration points and to the requirement of a new functional form.

The *J-R* curve obtained for the other two copolymeric materials are shown in Fig. 9, considering no crack tip blunting and a crack tip blunting with $m_{pcf} = \sqrt{3}$. The experimental points obtained by the multiple specimen method are also shown.

As observed in a previous study about unfilled PP copolymers [1], the quantification of crack tip blunting is a very important parameter during the application of the normalization method. In this sense, considering that there is no crack tip blunting results in a more optimistic resistance curve, due to the under-estimation of crack length during separable blunting region. This results in a higher value of *J*-integral at low values of crack length increment, but also in a lower resistance to

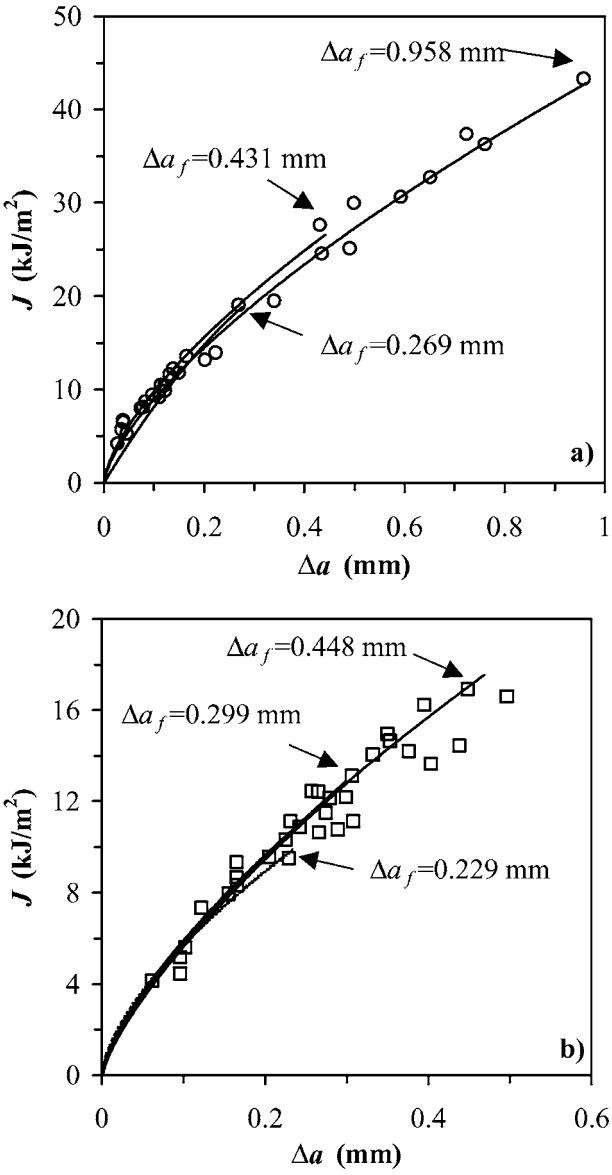

Figure 10 Resistance curves of (a) BPP and (b) B40H5L obtained with several fracture tests carried out up to different final crack extension levels. Closed symbols correspond to the multiple specimen data.

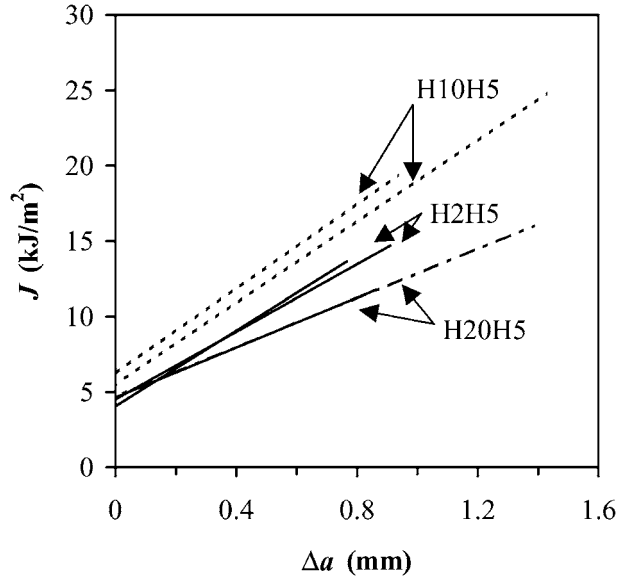

Figure 11 Resistance curve of the unfilled and filled materials based on homopolymer PP. For each material, two curves obtained from test performed up to different crack extension levels are shown.

crack growth once crack propagation has started. If fact, as the final point used during the power law fit of the normalized load variations is uninfluenced by the crack tip blunting quantification, the different *J-R* curves converge to the same point at high values of crack length increment. Since the initial part of the curve obtained without taking in account crack tip blunting presents higher value of J than that obtained considering m_{pcf}, the resulting slope of the resistance curve is lower.

The curves obtained considering crack tip blunting are in good agreement with the multiple specimen resistance curves, for both materials. This indicates that crack tip blunting has been adequately quantified and introduced in the normalization method. The *J-R* curves obtained by the normalization method from several specimens of different final crack length increments are shown in Fig. 10.

It can be observed that the different resistance curves coincide well in the common range of Δa, independently of the final crack length increment. This observation confirms the goodness of the normalization method and may be a manner to check the validity of a *J-R* curve obtained by the normalization method without the necessity to compare it with the curve obtained by the multiple specimen method.

The normalization method is applied to the determination of the *J-R* curve of the homopolymer PP-based materials. In this case, and as no multiple specimen information was available, the influence of crack tip blunting upon the normalization method application is reduced using a shorter separable blunting region and a value of $m_{pcf} = \sqrt{3}$. In the case of the materials filled with 40 wt% and 60 wt% of Magnifin H5 (H40H5 and H60H5), the *J-R* curve cannot be obtained due to an excessive decrease of the value of P once crack propagation initiation is reached, in the same manner than reported earlier for the 60 wt% filled block copolymer (B60H5L). The deformation function of these materials cannot be determined. In the case of lower mineral content, the calibrations points can be correctly fitted by a power law equation. The resistance curves of the materials based on homopolymer PP are shown in Fig. 11.

For all the materials, the resistance curves obtained with two samples tested up to different displacement levels are highly consistent. In the case of the 10 wt% material, however, a slight difference was observed between the two *J-R* curves. This divergence of the results is of the same order as the difference that can be obtained using the multiple specimen method and is due to experimental error associated with specimen geometry, internal defects, . . . The evolution of the *J-R* curve with the filler content is similar to that reported by Vu-Khanh *et al.* [24] for mica-filled polypropylene: The fracture resistance of the material is increased by a filler addition of up to 10 wt%. Above this concentration, the resistance decreases with filler content.

In order to find an explanation for the non-applicability of the normalization method for H40H5, H60H5 and B60H5L, the geometry of the plastic zone

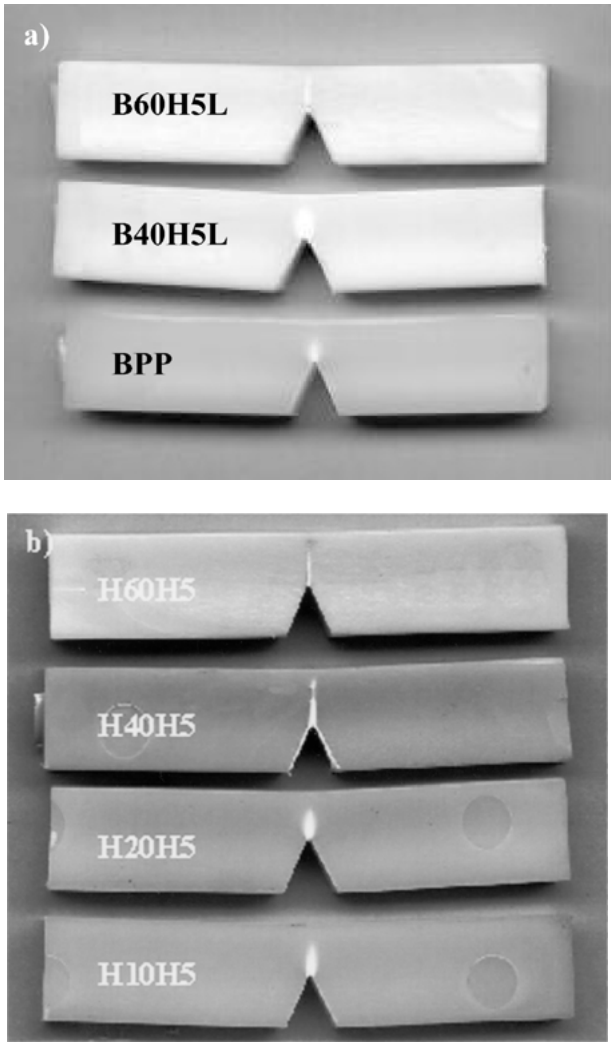

Figure 12 Observation of the plastic zone of the tested blunt-notched specimens. (a) BPP and (b) HPP based compounds.

of all the tested specimens is shown in Fig. 12. It is worth noting that the geometry observed at the surface of the sample may not be similar to that of the plastic zone at the center of the notch. The materials that are suitable for normalization method utilization present a circular plastic deformation zone ahead of the crack tip, meanwhile the other three materials show a narrow plastic zone, which extend along the whole ligament.

In particulate-filled polypropylenes, the two main mechanisms of plastic deformation are the shear yielding of the matrix and the debonding at the particle/matrix interface [25]. As was reported in another study about the compounds based on block copolymer PP [17], the filler particles act as internal defects in the polymer and promote debonding contribution to plastic deformation, limiting in the same time the plastic flow, i.e. the shear yielding of the matrix. This effect of the filler particle on the plastic deformation can be observed in Fig. 13, where the fracture surfaces of the copolymer-based materials are shown.

As filler content increased, the number of stretched polymeric fibrils increases but their final deformation level is reduced. The plastic deformation of the highly filled material results thus in a craze-like morphology where the material is still holding the applied tension through a few stretched polymeric fibrils. In this sense, it can be said that the plastic deformation and the crack propagation are not completely separated processes. This shows that load separation is not valid for these materials since the extension of load separability to growing cracks is limited by the condition that crack starts growing once plastic deformation pattern has fully developed [7]. It appears thus that load separation is not valid for highly filled materials. On the other hand, the use of a copolymeric matrix and of a surface-treated filler results in the shift of this transition between separable and unseparable behaviors to higher filler content. Two mechanisms contribute to the development of the plastic zone: the higher plastic deformation due to the lower yield strength of the copolymeric matrix and the lower extent of the interface due to the lubricant surface coating.

It seems thus that the coincidence of narrow plastic zone and non-validity of load separation may be a possible manner to check the applicability of the load normalization method during the fracture test. Nevertheless, more experimental evidence is required in order to consider this criterion of load separation.

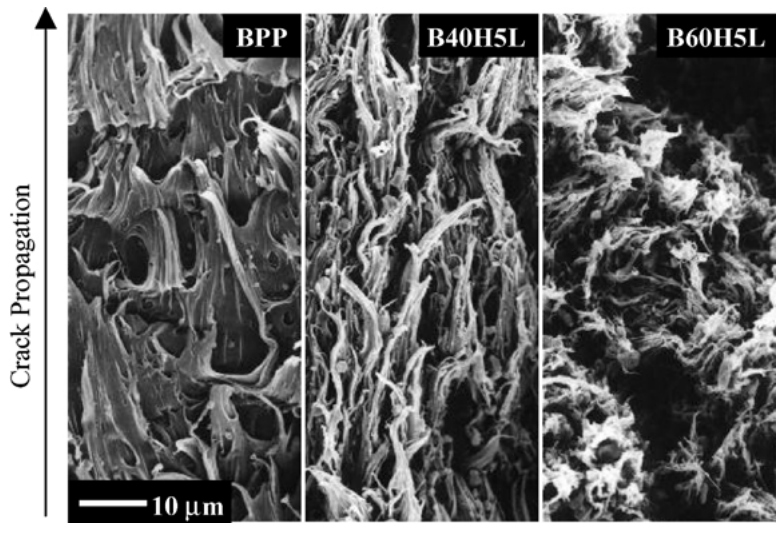

Figure 13 Fracture surface of the unfilled and filled copolymer PP, showing the matrix ductile tearing.

6. Conclusions

Load normalization method was applied to magnesium hydroxide filled polypropylenes. In this aim, the validity of load separation was studied using the criterion proposed by Sharobeam and Landes. It was checked that load can be written in a separable form as long as the condition of stationary crack length is fulfilled. In the case of heavily filled materials (60 wt%), crack propagation starts during the region of no-separation and the load separation validity was not checked. The geometry function, $G(a/W)$, was determined. The obtained value of η_{pl} was in good agreement with the theoretical value for the SENB geometry except for the material filled with high concentrations of mineral filler, for which it was slightly lower.

The deformation function was determined through the application of the load normalization method. A power law fit was used. In the case of heavily filled materials, it was observed that the method was not applicable due to the lack of separable blunting region and to the requirement of another functional form of $H(v_{pl}/W)$. The *J-R* curve can be plotted for the material with lower content of filler and a good concordance with the curve obtained by the multiple specibreak men method was observed. It has been found that the crack tip blunting has to be introduced in the procedure of the method, using the blunting line equation and a plastic constraint factor of $m_{pcf} = \sqrt{3}$. It was observed that the resistance curve was independent of the final extent of crack length and it was suggested that this observation is a mean of checking the consistence of the normalization method. Finally, it was observed that the normalization method applicability for a material coincide with circular plastic zone shape (observed at the surface of the sample), meanwhile a narrow plastic zone was observed for materials unsuitable for load normalization method.

Acknowledgment

C. Morhain thanks the CIRIT (Generalitat de Catalunya, Spain) for the concession of a predoctoral grant.

References

1. C. MORHAIN and J. I. VELASCO, *J. Mat. Sci.* **36** (2001) 1487.
2. J. R. LANDES and R. HERRERA. *Int. J. Fract.* **36** (1988) R9.
3. J. R. RICE, *J. Appl. Mech.* **35** (1968) 379.
4. J. R. BEGLEY and J. D. LANDES, in "Fracture Toughness," STP 514 (ASTM, Philadelphia, 1972) p.1.
5. V. KUMAR, M. D. GERMAN and C. F. SHIH, EPRI Report NP1931 (1981).
6. M. H. SHAROBEAM and J. D. LANDES, *Int. J. Fract.* **47** (1991) 81.
7. *Idem.*, *ibid.* **59** (1993) 213.
8. J. D. LANDES and Z. ZHOU, *ibid.* **63** (1993) 383.
9. C. R. BERNAL, P. E. MONTEMARTINI and P. M. FRONTINI, *J. Polym. Sci., Part B: Polym. Phys.* **34** (1996) 1869.
10. C. BERNAL, A. CASSANELLI and P. FRONTINI, *Polymer* **37** (1996) 4033.
11. C. BERNAL, M. RINK and P. FRONTINI, *Macromol. Symp.* **147** (1999) 235.
12. C. R. BERNAL, A. N. CASSANELLI and P. M. FRONTINI, *Polym. Test.* **14** (1995) 85.
13. V. GARCIA BROSA, C. BERNAL and P. FRONTINI, *Engng. Fract. Mech* **62** (1999) 231.
14. R. HERRERA and J. D. LANDES, in "Fracture Mechanics: Twenty-First Symposium," STP 1074 (ASTM, Philadelphia, 1990) p. 24.
15. T. W. ORANGE, in "Fracture Mechanics: Twenty-first Symposium," STP 1074 (ASTM, Philadelphia, 1990) p. 545.
16. ESIS Technical Committee 4, "A testing protocol for conducting *J-R* curve test on plastics" (European Structural Integrity Society, March 1991).
17. J. I. VELASCO, C. MORHAIN, D. ARENCÓN, O. O. SANTANA and M. L. MASPOCH, *Polymer Bulletin* **41** (1998) 615.
18. P. M. FRONTINI and A. FAVE, *J. Mater. Sci.* **30** (1995) 2446.
19. I. NARISAWA, *Polym. Engng. Sci.* **27** (1987) 41.
20. ASTM E 1152-87, in "Annual Book of ASTM Standards," Part 10 (ASTM, Philadelphia, 1987) p. 825.
21. J. I. VELASCO, J. A. DE SAJA and A. B. MARTINEZ, *Fatigue. Fract. Engng Mat. Struct.* **20** (1997) 659.
22. ASTM E813-87, in "Annual Book of ASTM Standards," Part 10 (ASTM, Philadelphia, 1987) p. 686.
23. G. R. IRWIN and P. C. PARIS, in "Fracture, an Advanced Treatise," Vol. 3, edited by H. Libowitz (Academic Press, New York, 1971) p. 13.
24. T. VU-KHANH, B. SANSCHAGRIN and B. FISA, *Polymer Composites* **6** (1985) 249.
25. A. J. KINLOCH and R. J. YOUNG, in "Fracture Behavior of Polymers" (Elsevier, London, 1983).

Received 15 January
and accepted 18 September 2001